Elastic turbulence in a polymer solution flow

Alexander Groisman and Victor Steinberg

Department of Physics of Complex Systems, Weizmann Institute of Science, Rehovot 76100, Israel

(February 4, 2008)

Turbulence is one of the most fascinating phenomena in nature and one of the biggest challenges for modern physics. It is common knowledge that a flow of a simple, Newtonian fluid is likely to be turbulent, when velocity is high, viscosity is low and size of the tank is large [1,2]. Solutions of flexible long-chain polymers are known as visco-elastic fluids [3]. In our experiments we show, that flow of a polymer solution with large enough elasticity can become quite irregular even at low velocity, high viscosity and in a small tank. The fluid motion is excited in a broad range of spatial and temporal scales. The flow resistance increases by a factor of about twenty. So, while the Reynolds number, Re, may be arbitrary low, the observed flow has all main features of developed turbulence, and can be compared to turbulent flow in a pipe at $\mathrm{Re} \simeq 10^5$ [1,2]. This *elastic turbulence* is accompanied by significant stretching of the polymer molecules, and the resulting increase of the elastic stresses can reach two orders of magnitude.

Motion of simple, low molecular, *Newtonian* fluids is governed by the Navier-Stokes equation [1,2]. This equation has a non-linear term, which is inertial in its nature. The ratio between the non-linearity and viscous dissipation is given by the Reynolds number, $Re = VL/\nu$,where V is velocity, L is characteristic size and ν is kinematic viscosity of the fluid. When Re is high, non-linear effects are strong and the flow is likely to be turbulent. So, turbulence is a paradigm for a strongly non-linear phenomenon [1,2].

Solutions of flexible high molecular weight polymers differ from Newtonian fluids in many aspects [3]. The most striking elastic property of the polymer solutions is that stress does

not immediately become zero when the fluid motion stops, but rather decays with some characteristic time, λ, which can reach seconds and even minutes. Equation of motion for dilute polymer solutions differs from the Navier-Stokes equation by an additional linear term due to the elastic stress, τ [3]. Since the elastic stress is caused by stretching of the polymer coils, it depends on history of motion and deformation of fluid elements along its flow trajectory. This implies non-linear relationship between τ and the rate of deformation in a flow [3]. The *non-linear mechanical properties* of polymer solutions are well manifested in their large extensional viscosity at high rates of extension [4] and in the Weissenberg effect [5,3]. Degree of non-linearity in the mechanical properties is expressed by the Weissenberg number, $Wi = V\lambda/L$, which is a product of characteristic rate of deformation and the relaxation time, λ.

It is reasonable to inquire, whether non-linearity of mechanical properties of a fluid can give rise to turbulent flow, when the equation of motion is linear. For a polymer solution this corresponds to a state, when the Weissenberg number is large, while the Reynolds number is small. This situation can be realized, if the parameter of elasticity $Wi/Re = \lambda\nu/L^2$ is large enough. An important step in investigation of influence of the non-linear mechanical properties on flow was made about a decade ago, when *purely elastic* instability was experimentally identified in curvilinear shear flows [6,7]. This instability occurs at moderate Wi and vanishingly small Re and is driven by the elastic stresses [7,9]. As a result of the instability, secondary, in general oscillatory, vortex flows develop, and flow resistance somewhat increases [6–10]. Flow instabilities in elastic liquids are reviewed in [11,12].

There is no unique commonly accepted definition of turbulent flow [2], so it is usually identified by its major features [1,2]. Turbulence implies fluid motion in a broad range of spatial and temporal scales, so that many degrees of freedom are excited in the system. A striking practically important characteristic of turbulent flows is major increase in the flow resistance compared to an imaginary laminar flow with the same Re. Experiments that we report in this letter show, how these main features of turbulence appear in a flow of a highly elastic polymer solution at low Reynolds numbers.

For our experiments we chose swirling flow between two parallel disks, Fig.1, and a dilute solution of high molecular weight polyacrylamide in a viscous sugar syrup, as the working fluid. The curvature ratio was made quite high, $d/R = 0.263$, in order to provide destabilization of the primary shear flow and development of the secondary vortical fluid motion at lower shear rates [7,10]. (The flow between two plates with small d/R was studied before in context of the purely elastic instability [10].) The whole flow set-up was mounted on top of a commercial viscometer (AR-1000 of TA-instruments), so that we could precisely measure the angular velocity, ω, of the rotating upper plate and the torque applied to it. In this way we were able to estimate the average shear stress, σ, in the polymer solution and to compare it with the stress in the laminar flow, σ_{lam}, with the same applied shear rate. In Newtonian fluids the ratio σ/σ_{lam} generally grows with Re as the flow becomes increasingly irregular, and the magnituide of σ/σ_{lam} can be considered as a measure of strength of turbulence and turbulent resistance. In our set-up σ becomes 30% higher than σ_{lam} at $Re = 70$, that can be regarded as a point when inertial effects become significant.

Dependence of σ/σ_{lam} on the shear rate, $\dot{\gamma} = \omega R/d$, for flow of the polymer solution in the experimental system is shown in Fig.2 (first curve). One can see that at $\dot{\gamma}$ of about 1 s^{-1} (corresponding to $Wi \equiv \lambda\dot{\gamma} = 3.5$) a sharp transition occurs that appears as a significant increase in the apparent viscosity. The Reynolds number at the transition point is about 0.3, so that the inertial effects are quite negligible there. The transition has pronounced hysteresis, which is typical for the purely elastic flow instability [9]. The ratio σ/σ_{lam} keeps growing with the shear rate and at the highest $\dot{\gamma}$, that has been reached, the flow resistance is about 12 times larger than in the laminar flow. In the same range of shear rates, flow of the pure solvent is completely laminar and the ratio σ/σ_{lam} is unity within resolution of the viscometer (about 1%). To make sure, that the observed flow phenomena were indeed caused by the solution elasticity, we measured σ for a few solutions with the same polymer concentration, but different relaxation times, λ. The curves of σ/σ_{lam} coincided, when plotted against Wi, while the Reynolds number turned out to be completely irrelevant (see also [9]). The growth of the resistance in the polymer solution flow becomes even larger,

when the size of the gap is increased (2nd curve in Fig.2). Then the ratio σ/σ_{lam} reaches a value of 19. Such growth of the flow resistance is found for Newtonian fluids in the same flow geometry at Re of about $2{\cdot}10^4$. For flow in a circular pipe this value of σ/σ_{lam} is reached at $Re \simeq 10^5$, which is usually considered as a region of rather developed turbulence [1].

Two representative snapshots of the polymer solution flow above the transition (at $\dot{\gamma} = 4$ s^{-1}) are shown in Fig.3. One can see that the flow patterns are very much irregular and structures of quite different sizes appear. This visual impression is confirmed by a more careful analysis. In Fig. 4 one can see average Fourier spectra of the brightness profiles along the diameter and along the circumference. The both spectra exhibit power law decay over a decade in the vawenumber domain.

Characteristic time spectra of velocity fluctuations at different shear rates are shown in Fig. 5. Flow velocity was measured in the horizontal plane in the center of the set-up, where its average value is zero. As the shear rate is raised, the power of fluctuations increases and characteristic frequencies become higher. On the other hand, the general form of the spectra remains very much the same. In particular, just like for the spatial spectra in Fig. 4, there is a region of a power law decay, which spans over about a decade in frequencies. This power law dependence in the broad ranges of spatial and temporal frequencies actually means that the fluid motion is excited at all those spatial and temporal scales. Spectra of radial and azimuthal velocities taken at different points with non-zero average flow had the same general appearance and close values of exponents in the power law decay range.

Summarizing all the results, we conclude that the flow of the elastic polymer solution at sufficiently high Wi has indeed all main features of developed turbulence. By the strength of the turbulent resistance, and by the span of scales in space and time, where the fluid motion is excited, the observed flow can be compared to turbulence in a Newtonian fluid in a pipe at Re of about 10^5. This apparently turbulent flow arises solely due to non-linear mechanical properties of the elastic polymer solutions. So, we called the phenomenon *elastic turbulence*, in contrast to the usual inertial turbulence which is observed in Newtonian fluids at high Re. (The name "elastic turbulence" has been used before for designation of apparently

disordered flows in polymeric liquids [13]. No attempt has been ever made,however, to characterize those flows quantitatively.)

The elastic turbulence has many features that are in sharp contradiction to the intuition based on the Newtonian fluid mechanics. So, velocity required for excitation of inertial turbulence in a Newtonian fluid is proportional to the fluid viscosity. On the other hand, the polymer relaxation time, λ, usually grows proportionally to the viscosity. Since at constant d/R transition to elastic turbulence occurs at a certain value of the Weissenberg number, $Wi = V\lambda/L$, choosing more viscous polymer solutions, one can excite turbulence at lower velocities. Indeed, using a solution of polymers in a very viscous sugar syrup, we observed transition to the elastic turbulence at a rotation rate of 0.05 s^{-1} (corresponding to $Re = 10^{-2}$). Further, in an elastic polymer solution the scale of time, λ, does not depend on the size of the system. Therefore, as long as the ratio d/R is preserved, transition to turbulence should occur at the same ω and the dependence of σ/σ_{lam} on $\dot{\gamma}$ should not change with the size of the system. We repeated the measurements of σ in a small set-up having all the dimensions reduced by a factor of 4 compared to the standard system. The dependence of σ/σ_{lam} on $\dot{\gamma}$ was found to be the same (the data are not shown) as in Fig.2, while the characteristic velocities and the Reynolds numbers were lower by factors of 4 and 16, respectively. Therefore, we believe that using polymer solutions with sufficiently high elasticity, we can excite turbulent motion at arbitrary low velocities and in arbitrary small tanks. (The size of the tank still has to be large, compared to the size of the polymer coils.)

An important question about the elastic turbulence is, where the turbulent resistance comes from. In the inertial turbulence the origin of the large resistance is the Reynolds stress, which is connected with high kinetic energy of the turbulent motion and takes major part in the momentum transfer in the flow. Elastic turbulence occurs at low Reynolds numbers. From our velocity measurements in the standard set-up, contribution of the Reynolds stress to the flow resistance could be estimated as being less than 0.5%. The contribution of the viscous shear stress of the Newtonian solvent, averaged across the fluid layer, is always the same as in laminar flow and cannot change. Thus, the whole increase in the flow resistance

should be due to the elastic stress. The data shown in Fig.2 (2nd curve) imply that the polymer contribution to the stress increases by a factor of up to 65, compared to laminar flow with the same average shear rate. This suggestion agrees very well with our measurements of relaxation of the shear stress after the fluid motion is stopped. The elastic part, τ, of the whole stress, is identified by its slow relaxation with a characteristic time of the order λ. In the elastic turbulence this slowly relaxing part can become two orders of magnitude larger than in the laminar flow with the same shear rate. This major growth of the elastic stress should be connected with vast extension of the polymer molecules in the turbulent flow.

Thus, the scenario of development of the elastic turbulence is apparently the following. The polymer molecules are stretched in the primary shear flow, drive it unstable and cause irregular secondary flow. The flow acts back on the polymer molecules stretching them further and becomes increasingly turbulent, until a kind of saturated dynamic state is finally reached. Density of the elastic energy of the stretched polymers can be estimated as $Wi \cdot \tau/2$. So, it should increase in the elastic turbulent flow by about the same factor as the elastic stress, τ, while the kinetic energy is always quite small.

Methods. We used solution of 65% saccharose, 1% NaCl in water, viscosity $\eta_s = 0.324$ Pa·s, as a solvent for the polymer. We added polyacrylamide (M_w=18,000,000, Polysciences) at a concentration of 80 ppm by weight. The solution viscosity was $\eta = 0.424$ Pa·s at $\dot{\gamma} = 1$ s^{-1}. The relaxation time, λ, estimated from the phase shift between the stress and the shear rate in oscillatory tests, was 3.4 s.

REFERENCES

[1] Landau L. D. and Lifschitz, E. M., *Fluid mechanics*, Pergamon Press , Oxford, 1987.

[2] Tritton D. J., *Physical Fluid Dynamics*, Clarendon Press, Oxford, 1988.

[3] Bird, R. B., Curtiss, C. F., Armstrong, R. C., and Hassager, O., *Dynamics of polymeric liquids*, John Wiley, NY, 1987.

[4] Tirtaatmadja, V. and Sridhar, T. A filament stretching device for measurement of extensional viscosity, *J. Rheology* **37**, 1081-1102 (1993);

[5] Weissenberg, K., A continuum theory of rheological phenomena, *Nature* **159**, 310-311 (1947).

[6] Magda, J. J. and Larson, R. G., A transition occuring in ideal elastic liquids during shear flow, *J. Non-Newtonian Fluid Mech.* **30**, 1-19 (1988).

[7] Muller, S. J., Larson, R. G. and Shaqfeh, E. S. G. A purely elastic transition in Taylor-Couette flow, *Rheol. Acta* **28**, 499-503 (1989).

[8] Larson, R. G., Shaqfeh, E. S. G., and Muller, S.J. A purely viscoelastic instability in Taylor-Couette flow, *J. Fluid Mech.* **218**, 573-600 (1990).

[9] Mechanism of elastic instability in Couette flow of polymer solutions: experiment,*Phys. Fluids* **10**, 2451-2463 (1998).

[10] Byars J. A., Öztekin, A., Brown R. A. and McKinley G. H., Spiral instabilities in the flow of highly elastic fluids between rotating parallel disks, *J. Fluid Mech.* **271**, 173-218 (1994)

[11] Larson, R. G., Instabilities in viscoelastic flows, *Rheol. Acta* **31**, 213-263, (1992)

[12] Shaqfeh, E. S. G., Purely elastic instabilities in viscometric flows, *Annu. Rev. Fluid Mech.* **28**, 129-185 (1996).

[13] Giesekus, H. W., Non-linear effects in the flow of visco-elastic fluids through slits and holes, *Rheol. Acta* **7**, 127-138, (1968).

Figure captions

Fig.1 Schematic drawing of the experimantal set-up. The set-up consists of a stationary cylindrical cup with a plain bottom (the lower plate), which is concentric with the rotating upper plate. The latter is attached to the shaft of a commercial rheometer. The radii of the upper and the lower plates are R=38 mm and R_2=43.6 mm, respectively. The liquid is filled till a level d, which is 10 mm, if not stated differently. The upper plate just touches the surface of the liquid. A special cover is put from above to minimize evaporation of the liquid. The temperature is stabilized at 12 °C by circulating water under the steel lower plate. The walls of the cup are transparent that allows to make laser Doppler velocimeter measurements by collecting light scattared from the crossing point of two horizontal laser beams. In the experimental runs, where the flow has to be viewed from below, the lower plate is made from plexiglass and a mirror tilted by 45° is placed under the lower plate. Then the flow patterns are captured by a CCD camera from a side and the temperature is stabilized by circulating air in a closed box.

Fig.2 The ratio of the average stress, σ, measured in the flow, to the stress, σ_{lam}, in the laminar flow with the same boundary conditions, as a function of the shear rate, $\dot{\gamma}$. The curves 1 and 2 are for the polymer solution flow with the gap between the plates $d = 10$ mm and 20 mm, respectively. The shear rate was gradually varied in time, very slowly (by about 10% per hour) in the transition region, and faster below and above it. Thin black lines are for increasing $\dot{\gamma}$, while thick gray lines correspond to lowering of $\dot{\gamma}$. The curve 3 is for the pure solvent. Mechanical degradation of the polymers was quite small at shear rates below 1.5 s^{-1} and 1 s^{-1} for $d = 10$ mm and 20 mm, respectively. So, the dependences of σ/σ_{lam} on $\dot{\gamma}$ in those regions were reproducible in consecutive runs within about 1%. Degradation effects became appreciable at higher shear rates, and elasticity typically decreased by up to 10% as a result of the runs shown by the curves 1 and 2.

Fig.3 Two snapshots of the flow at $Wi = 13$, $Re = 0.7$. The flow under the black upper plate is visualized by seeding the fluid with light reflecting flakes (1% of the Kalliroscope liquid). The fluid is illuminated by ambient light. Although the pattern is quite irregular, one can see that appearing structures tend to have spiral-like form. The dark spot in the middle corresponds to the center of a big persistent thoroidal vortex that has dimensions of the whole set-up.

Fig.4 Average Fourier spectra of the brightness profiles taken along the diameter (thin black line) and along the circumference at a radius of $2d$ (thick gray line). The averaging was made over long series of flow pattern snapshots taken in consecutive moments of time. The wavelength is measured in units of d, so that the wavenumber, k, of unity corresponds to a length of $2\pi d$. The spectrum taken along the diameter apparently differs from the azimuthal spectrum by a series of broad peaks. This may be a manifestation of the fact, that the flow is not completely structureless and homogeneous along the radial direction (see Fig.3). The visualization method we used (Fig. 3) does not provide direct information about the fluid velocity. So, the specific value of the exponent in the power law fit, $A \sim k^{-1}$, should not be given much consideration to.

Fig.5 Power spectra of velocity fluctuations in the standard set-up at different shear rates, $\dot{\gamma}$. The fluid velocity was measured by a laser Doppler velocimeter in the center of the flow. The curves 1 - 5 correspond to $\dot{\gamma}$=1.25, 1.85, 2.7, 4, and 5.9 s^{-1}, respectively (all above the transition point $\dot{\gamma} \simeq 1$, Fig.2). The power, P, of fluctuations is fitted by a power law, $P \sim f^{-3.5}$, for $\dot{\gamma} = 4s^{-1}$ over about a decade in frequencies, f.

Acknowledgement. Support of the Minerva Center for Nonlinear Physics of Complex Systems is gratefully acknowledged.

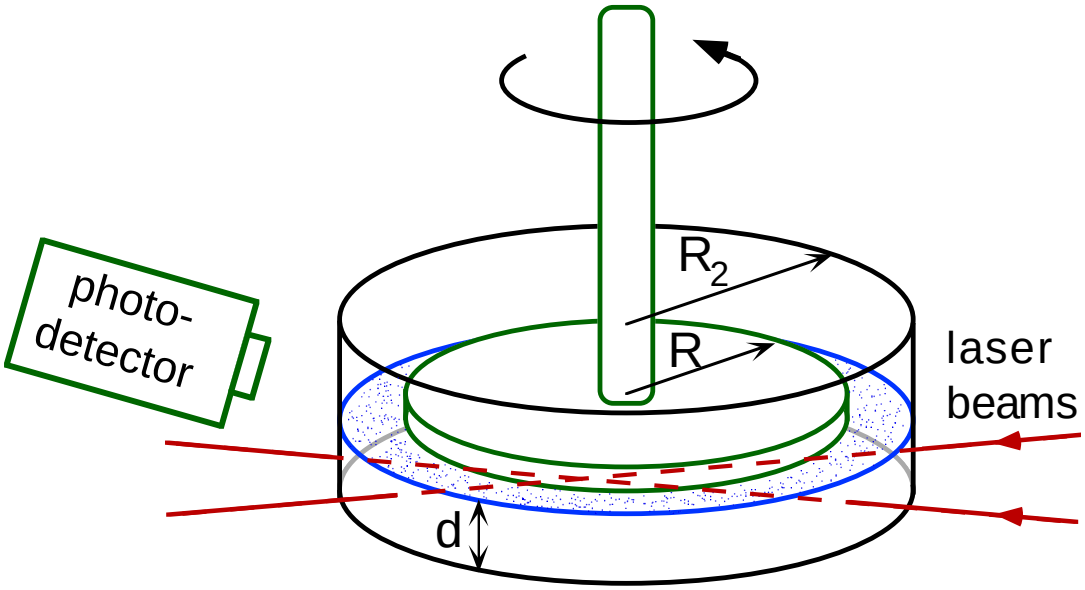
photo-
detector
R2
R
laser
beams
d

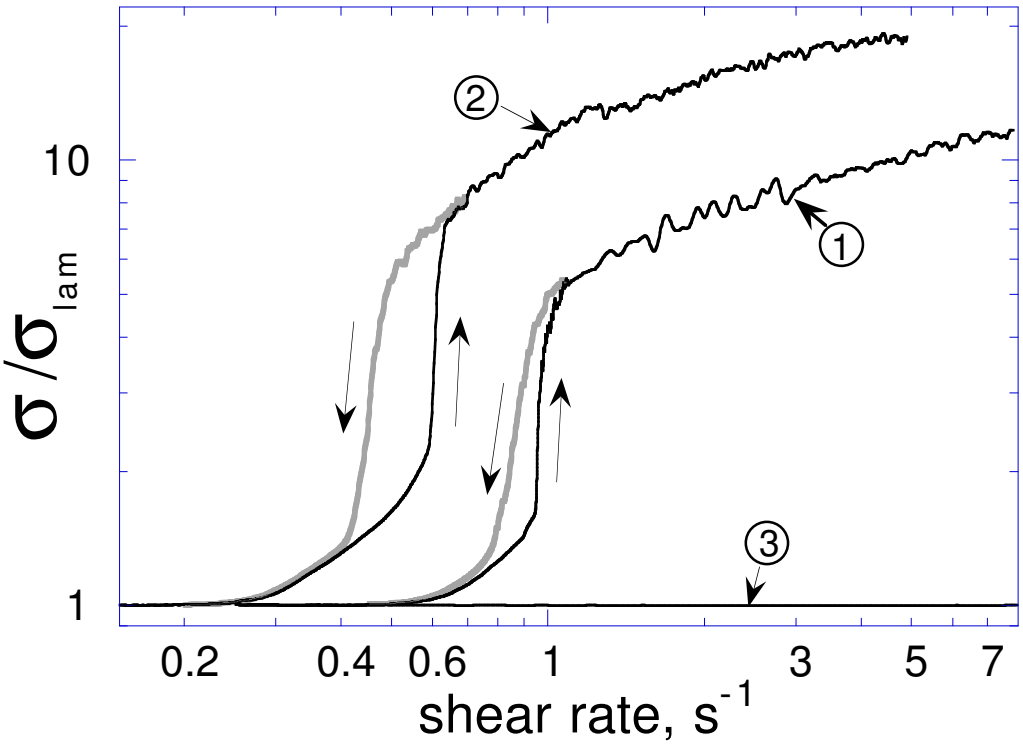
10
1
σ /σ lam
0.2
0.4
0.6
1
3
5
7
shear rate, s-1
①
②
③

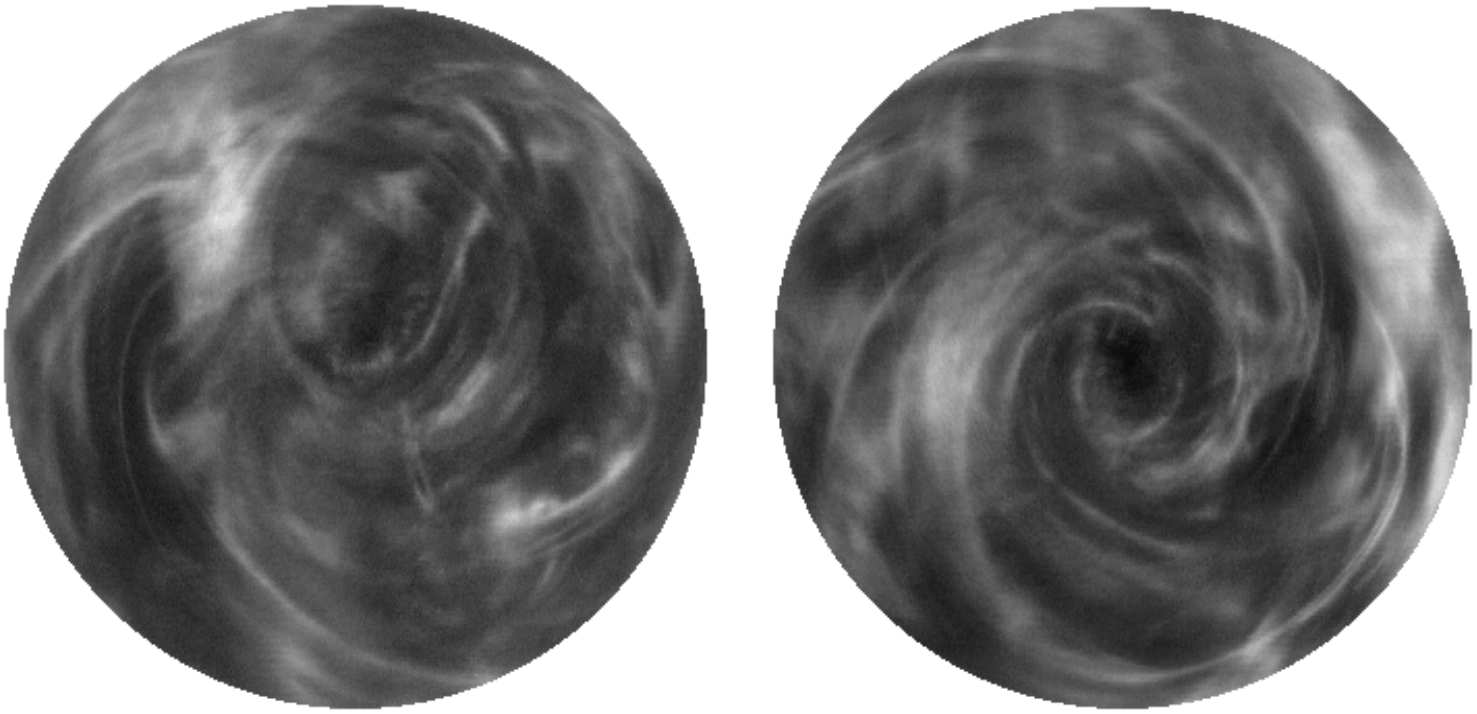

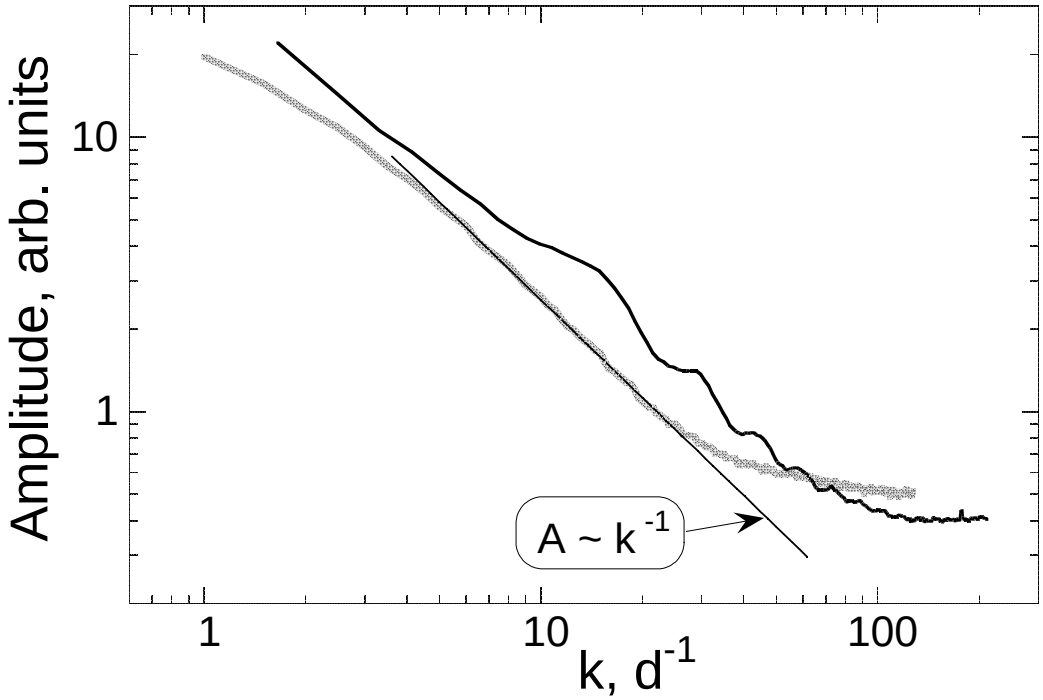
Amplitude, arb. units
10
1
1
10
100
k, d-1
A ~ k -1

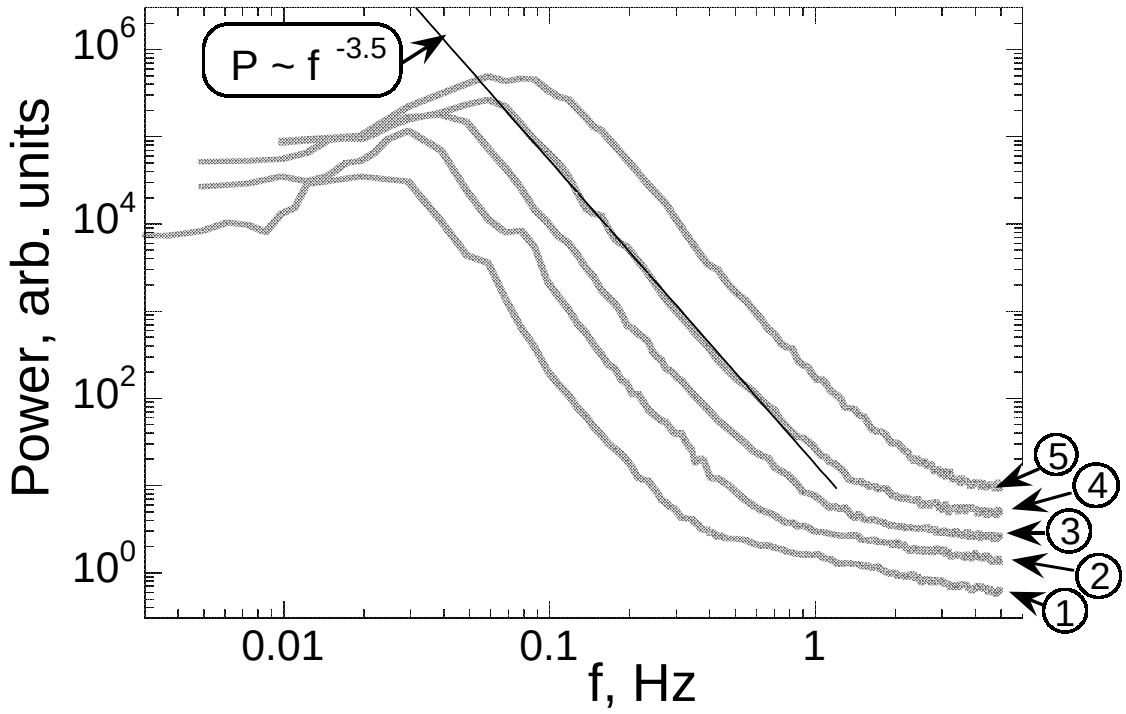
P ~ f -3.5
Power, arb. units
10^6
10^4
10^2
10^0
0.01
0.1
1
f, Hz
5
4
3
2
1